Applied Catalysis B: Environmental 121–122 (2012) 10–19

Contents lists available at SciVerse ScienceDirect

Applied Catalysis B: Environmental

journal homepage: www.elsevier.com/locate/apcatb

A lumped kinetic model based on the Fermi's equation applied to the catalytic wet hydrogen peroxide oxidation of Acid Orange 7

Adrián M.T. Silva[a], J. Herney-Ramirez[b,c], Umut Söylemez[d], Luis M. Madeira[b,*]

[a] LCM - Laboratory of Catalysis and Materials - Associate Laboratory LSRE/LCM, Faculdade de Engenharia, Universidade do Porto, Rua Dr. Roberto Frias, 4200-465 Porto, Portugal
[b] Laboratório de Engenharia de Processos, Ambiente e Energia (LEPAE), Departamento de Engenharia Química, Faculdade de Engenharia, Universidade do Porto, Rua Dr. Roberto Frias s/n, 4200-465 Porto, Portugal
[c] Universidad Nacional de Colombia, Facultad de Ingeniería, Departamento de Ingeniería Química y Ambiental, Carrera 30 No 45-03, Bogotá, DC, Colombia
[d] Department of Chemical Engineering, Faculty of Engineering, Ege University, Bornova, Izmir, Turkey

ARTICLE INFO

Article history:
Received 12 January 2012
Received in revised form 14 March 2012
Accepted 20 March 2012
Available online 28 March 2012

Keywords:
Acid Orange 7 (Orange II)
Catalytic wet hydrogen peroxide oxidation
Fe-containing pillared clay
Reaction kinetic model
Fermi's equation
Total organic carbon

ABSTRACT

A catalytic wet hydrogen peroxide process was applied for the degradation of an azo dye – Acid Orange 7, also called Orange II (OII) – using as catalyst a pillared saponite clay impregnated with 21 wt.% of iron. Tests were carried out in a slurry batch reactor, following along time the OII degradation, the dye mineralization and the iron leaching from the support. A detailed parametric study was done, changing one variable at a time, while keeping the others constant. Among the variables studied (temperature, catalyst dose, and initial concentration of oxidant – H_2O_2 – or dye), temperature revealed to have a marked effect, increasing reaction rate but also iron leaching from the support (which was in all cases still negligible, thus allowing to comply with legislated standards and evidencing the heterogeneous character of the process). A previously developed semi-empirical kinetic model, based on the Fermi's equation (the mirror image of the logistic function), was used to successfully describe the evolution of the OII concentration in this complex process. Such equation was extended in the present work by developing a lumped model proposed to predict the evolution of the total organic carbon along time; this model also showed very good adherence to the experimental data.

1. Introduction

Large amounts of dyes-containing waste waters are generated in several industrial processes, including textile, leather, paper and plastic processing, among others, being estimated that over 7×10^5 tonnes of dyestuff are produced annually [1–5]. For this reason, different methods have been studied to treat waste waters polluted with dyes, e.g., adsorption [6], adsorption/precipitation [7], electro-coagulation [8,9], oxidative degradation [10] and biochemical degradation [11]. However, most of them are limited by the respective costs and effective application; this is the case of biological processes, due to the non-biodegradable nature of some dyes, although the technology is cost-attractive. Non-catalytic and catalytic ozonation [12,13], catalytic wet peroxide oxidation [14,15], photocatalytic [16,17], electrochemical [18] and Fenton processes [19,20], besides other hydrogen peroxide (H_2O_2) assisted methods [21–25], are some of the already tested alternatives in the domain of the advanced oxidation processes (AOPs).

The Fenton/Fenton-like process, a particular case of the catalytic wet hydrogen peroxide oxidation (CWHPO), is usually operated at room temperature and ambient pressure and involves a strong reactive mixture of H_2O_2 and ferrous (Fe^{2+}) and/or ferric (Fe^{3+}) ions [26]. Several heterogeneous catalysts have been already developed with the aim to overcome the well known drawbacks of this process, namely the need to recover iron after the treatment and the need to operate in a limited pH range (3–4). One typical approach to develop such heterogeneous catalysts consists in the incorporation/deposition of iron on porous supports, such as zeolites [27,28], carbon materials [29–31] and clays [32–35]. In particular, pillared clays (PILCs in short) are materials of increasing interest because they are abundant natural minerals, with attractive properties and structures, that have already proved to be adequate supports to produce active and stable materials in aqueous media [25,36].

Recently, we have reported the effect of the main reaction conditions (temperature, catalyst load and both pollutant and H_2O_2 concentrations) on the heterogeneous CWHPO process for the treatment of a non-biodegradable azo-dye acid that has been widely used in several industries, i.e. the Orange 7 azo-dye (also known as Orange II – OII) [37]. A pillared saponite clay impregnated with Fe(II) acetylacetonate (~16 wt.% of iron) was used as catalyst because it was verified in a previous work [34] that a catalyst with

* Corresponding author. Tel.: +351 22 5081519; fax: +351 22 5081449.
E-mail address: mmadeira@fe.up.pt (L.M. Madeira).

0926-3373/$ – see front matter © 2012 Elsevier B.V. All rights reserved.
doi:10.1016/j.apcatb.2012.03.018

a similar nominal content (~17 wt.%) was the most stable for the Fenton process in terms of leaching of the active phase (<0.6 wt.% after 4 h), when compared to catalysts prepared with lower nominal contents (7.5 and 13 wt.% of Fe) or even when compared to catalysts prepared with other precursors of the active phase, such as Fe(II) oxalate, Fe(II) acetate and Fe(III) acetylacetonate. In addition, a simple semi-empirical kinetic model (based on the Fermi's equation and with a few adjustable parameters) was used to successfully describe the evolution of the OII concentration along time in such complex process [37].

In comparison with the commonly employed two-step pseudo-first-order model, kinetics based on Fermi's equation are very useful because with a single semi-empirical function it is possible to account for the dye concentration in the transition regime existing between the initial slow degradation of the pollutant (induction period) and the subsequent rapid concentration decay (inverted S-shaped transient curve), a behavior that has been often observed in AOPs [34,35,37–39].

The main aim and major novelty of the present work was to develop a lumped kinetic model, also based on the Fermi's equation, which permits to describe also the total organic carbon histories for the OII degradation by the CWHPO process and that to the best of author's knowledge was never reported before. A pillared saponite clay impregnated with Fe(II) acetylacetonate was used as catalyst, in line with the previous works [34,37], but in this particular case containing a higher nominal content of the active phase (21 wt.% of iron). In this way, the model developed for OII is extended, if validated, for pillared clays containing higher iron loads, which proved to be more active and stable [34,37]. In addition, the effect of iron content on the catalyst performance and kinetic parameters is evaluated.

2. Materials and methods

2.1. Catalyst preparation and characterization

The supported catalyst was prepared by a method reported in detail elsewhere [34], using Al-pillared saponite as support and Fe(II) acetylacetonate as precursor, being the conditions tuned with the aim of obtaining ca. 21 wt.% of iron in the catalyst. Briefly, the saponite clay, pillared with aluminum polycations by a standardized method, was impregnated (incipient wetness impregnation) with a solution of Fe(II) acetylacetonate in acetone. The obtained material was then calcined at 500 °C because it was previously found [34] that the organic moieties of the precursor were completely decomposed at this temperature.

The support and the obtained catalyst were characterized by several techniques, but since the data are comparable to those obtained in previous publications [34,37], in this work is only included the chemical composition of the prepared sample (Table 1) and attention was mostly focused on the kinetic modeling and on the operating parameters. Therefore, detailed information including equipment, conditions, procedures and respective characterization data for this kind of impregnated pillared saponite clay materials can be found in such previous works. The main difference between them is the nominal iron content, that in the present work is 21.04 wt.%, in close agreement with the targeted content, while the other quantified elements were Mg (10.63 wt.%), Al (5.33 wt.%), Si (21.25 wt.%), K (0.20 wt.%) and O (41.55 wt.%), as shown in Table 1.

2.2. Catalytic activity

The experimental setup and the respective experimental procedure for the degradation of OII (Orange II, Fluka p.a.) by CWHPO are also described elsewhere [37]. Briefly, 1 L of a OII solution with the desired concentration of the dye was placed in a jacketed glass batch reactor, together with the powder catalyst under continuous stirring and with a permanent control of temperature. The beginning of the reaction ($t = 0$) was considered when H_2O_2 (30%, w/w, from Merck) was injected. All the experiments were performed with an initial pH of 3.0, which has proven to be the optimum one for degradation of OII by this particular process [34] and has been also widely reported to be the optimum value for degradation of other organic pollutants [40].

The temperature, pH and OII concentration (determined by measuring the absorbance at $\lambda_{max} = 486$ nm in a Philips PU8625 UV/VIS spectrophotometer) were permanently measured during the experiments. The iron concentration in the liquid phase (assessed in an UNICAM 939/959 atomic absorption spectrophotometer) and the total organic carbon (TOC) content (Shimadzu 5000A analyser) were also assessed over time; for these analyses, the withdrawn samples were filtered (by means of 0.8 μm glass fiber paper) and an excess of Na_2SO_3 was immediately added to stop the reaction by consumption of the H_2O_2 remaining in the sample.

Tables 2 and 3 gather the conditions employed for all the performed experiments; Table 2 contains also kinetic data related with the OII concentration histories while Table 3 refers to results obtained with the TOC concentration histories. As can be observed, the experiments were conducted by varying the temperature (in the range 10–70 °C), the catalyst load (in the range of 20–100 mg L^{-1}), the initial concentration of the dye (between 0.02 and 0.2 mM), and the H_2O_2 dosage (between 3.0 and 48 mM).

It is important to refer that all experiments were conducted in chemical regime because neither external nor internal mass transfer resistances exist (proved by changing the stirring speed and the catalyst particle size, respectively, being obtained similar reaction rates in these conditions). Some experiments were repeated at least twice and the average absolute deviation between repeated runs was always less than 3%. It should be also remarked that the OII oxidation by using H_2O_2 without any catalyst, as well as the OII removal by adsorption (blank runs without H_2O_2), are practically negligible, as verified in previous works with iron-containing pillared clay materials and similar experimental conditions [34,39].

3. Results and discussion

3.1. Temperature effect

Fig. 1a and b show the results obtained for the OII and TOC degradation histories, respectively, at four different temperatures (10, 30, 50 and 70 °C). As expected, considering the Arrhenius law in the kinetic regime, the oxidation reaction in terms of both OII and TOC degradation accelerates when increasing the temperature. OII was completely degraded after 3 h of reaction regardless the reaction temperature used in the range of 30–70 °C (Fig. 1a), while there is a fraction of TOC remaining in the solution even at the end of the experiments, corresponding to 28.5, 20.0 and 17.1% of the initial TOC content for 30, 50 and 70 °C, respectively (Fig. 1b). Theoretically, 42 mol of H_2O_2 are needed to completely degrade 1 mol of the dye ($C_{16}H_{11}N_2NaO_4S + 42H_2O_2 \rightarrow 16CO_2 + 46H_2O + 2HNO_3 + NaHSO_4$) [41]. Therefore, the performances reached correspond to a theoretical efficacy of H_2O_2 usage of 50.1% at 30 °C, 56.0% at 50 °C and 58.0% at 70 °C.

For the lowest temperature (10 °C) the reaction slows down markedly and only 13 and 11% of OII and TOC are respectively degraded after 4 h of reaction. Along the experiment at 10 °C a similar trend was found for both OII and TOC concentration histories, suggesting that most of the TOC decrease is due to the OII and not to

Table 1
Chemical composition of the pillared saponite clay impregnated with Fe(II) acetylacetonate.

	Element					
	Fe	Mg	Al	Si	K	O
Average concentration (wt.%)	21.04	10.63	5.33	21.25	0.20	41.55

Table 2
Conditions employed in the runs performed, and kinetic parameters obtained after regression of the OII concentration histories (Eq. (1)); the corresponding coefficients of variation (CV) are also shown, as well as the determination coefficients (r^2).

T (°C)	C_{cat} (mg L^{-1})	$C_{H_2O_2}$ (mM)	C_{OII} (mM)	k (h^{-1})	k_{cv} (%)	t^* (h)	t^*_{CV} (%)	r^2
10	100	6.0	0.1	0.53	2.9	7.45	1.2	0.9743
30	100	6.0	0.1	2.90	2.6	1.33	2.7	0.9958
50	100	6.0	0.1	9.68	3.5	0.44	3.7	0.9959
70	100	6.0	0.1	25.3	6.4	0.13	6.9	0.9859
						Ea = 52 kJ mol^{-1}		0.9945
30	20	6.0	0.1	1.00	1.6	4.26	1.2	0.9948
30	40	6.0	0.1	1.70	0.9	2.31	0.9	0.9991
30	60	6.0	0.1	2.10	1.1	1.80	1.2	0.9990
30	80	6.0	0.1	2.53	1.0	1.73	1.0	0.9994
30	100	6.0	0.1	2.92	1.4	1.48	1.4	0.9989
						m = 0.66		0.9957
30	100	3.0	0.1	2.84	1.6	1.41	1.6	0.9985
30	100	6.0	0.1	2.90	2.6	1.33	2.7	0.9958
30	100	12	0.1	2.79	1.7	1.49	1.8	0.9982
30	100	24	0.1	2.68	1.5	1.48	1.5	0.9986
30	100	48	0.1	2.82	1.6	1.39	1.7	0.9984
						$j \sim 0$		–
30	100	6.0	0.02	3.38	1.6	0.82	1.7	0.9984
30	100	6.0	0.10	2.90	2.6	1.33	2.7	0.9958
30	100	6.0	0.20	1.76	1.1	1.87	1.2	0.9986
						n = −0.25		0.7460

the intermediates. In an experiment performed at the same temperature (10 °C) during 23 h (not shown), it was observed a continuous decrease of the OII concentration, being OII completely abated and 60.6% of the TOC removed; thus 39.4% of the initial TOC content remained in the solution at the end of the experiment.

Similar dependencies between the level of degradation achieved and the employed temperature were found in works reported with the CWHPO process and when using Fe-containing clays [35,37,39,42,43]. In addition, the obtained data indicate that among the reaction by-products formed during the OII degradation, some of them are non-oxidizable [44] and remain in the final solution under the employed conditions, because a plateau in TOC is observed for the three higher temperatures tested (Fig. 1b).

Considering the set of results at different temperatures, 30 °C might be considered satisfactory for the process because although the reaction is not as fast as at higher temperatures, a lower temperature might reduce the cost of the process and still has associated a significant performance. For this reason, this temperature was selected to perform the following runs where the other operating parameters were changed.

Table 3
Conditions employed in the runs performed, and kinetic parameters obtained after regression of the TOC concentration histories Eq. (2)); the corresponding coefficients of variation (CV) are also shown, as well as the determination coefficients (r^2).

T (°C)	C_{cat} (mg L^{-1})	$C_{H_2O_2}$ (mM)	C_{OII} (mM)	k_{TOC} (h^{-1})	$k_{CV,TOC}$ (%)	t^*_{TOC} (h)	$t^*_{CV,TOC}$ (%)	z_{TOC}	$z_{CV,TOC}$ (%)	r^2
10	100	6.0	0.1	0.54	10.8	6.64	5.4	0.39	2.2	0.9981
30	100	6.0	0.1	3.12	4.95	1.42	4.9	0.29	2.3	0.9989
50	100	6.0	0.1	9.08	7.57	0.49	7.7	0.22	3.1	0.9966
70	100	6.0	0.1	31.4	46.8	0.14	5.5	0.19	3.6	0.9906
							Ea = 54 kJ mol^{-1}			0.9952
30	20	6.0	0.1	1.21	13.9	3.42	6.1	0.65	10.3	0.9925
30	40	6.0	0.1	1.69	7.82	2.60	6.0	0.35	7.7	0.9970
30	60	6.0	0.1	2.03	5.12	1.97	4.6	0.30	3.7	0.9986
30	80	6.0	0.1	2.69	4.49	1.50	4.4	0.34	2.0	0.9996
30	100	6.0	0.1	3.12	4.95	1.42	4.9	0.29	2.3	0.9989
							m = 0.58			0.9777
30	100	3.0	0.1	3.11	6.23	1.44	6.1	0.29	2.8	0.9982
30	100	6.0	0.1	3.12	4.95	1.42	4.9	0.29	2.3	0.9989
30	100	12	0.1	3.13	5.06	1.42	5.0	0.29	2.3	0.9988
30	100	24	0.1	3.29	4.78	1.42	4.7	0.29	2.1	0.9990
30	100	48	0.1	3.26	4.87	1.41	4.8	0.28	2.2	0.9990
							$j \sim 0$			–
30	100	6	0.10	3.12	4.95	1.42	4.86	0.29	2.3	0.9990
30	100	6	0.20	2.72	11.4	2.33	10.6	0.33	6.5	0.9946
							n = −0.20			–

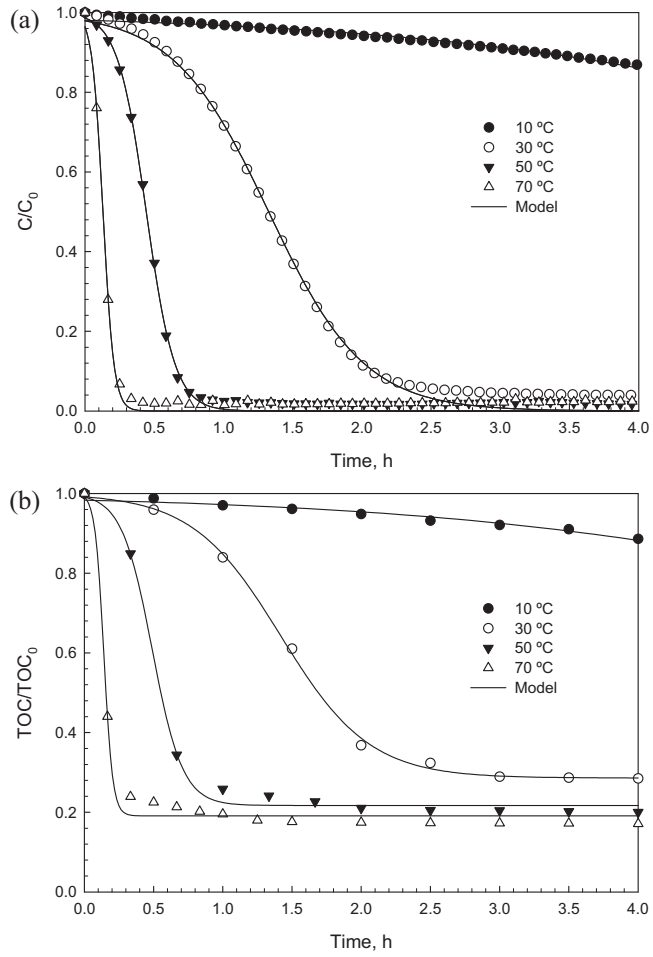

Fig. 1. Effect of temperature on the dye (a) and TOC (b) degradation histories (C_{cat} = 100 mg L^{-1}, $C_{H_2O_2}$ = 6 mM, C_{OII} = 0.1 mM). The lines represent the fitting by the model (Eqs. (1) and (2) respectively in (a) and (b) with data reported in Tables 2 and 3).

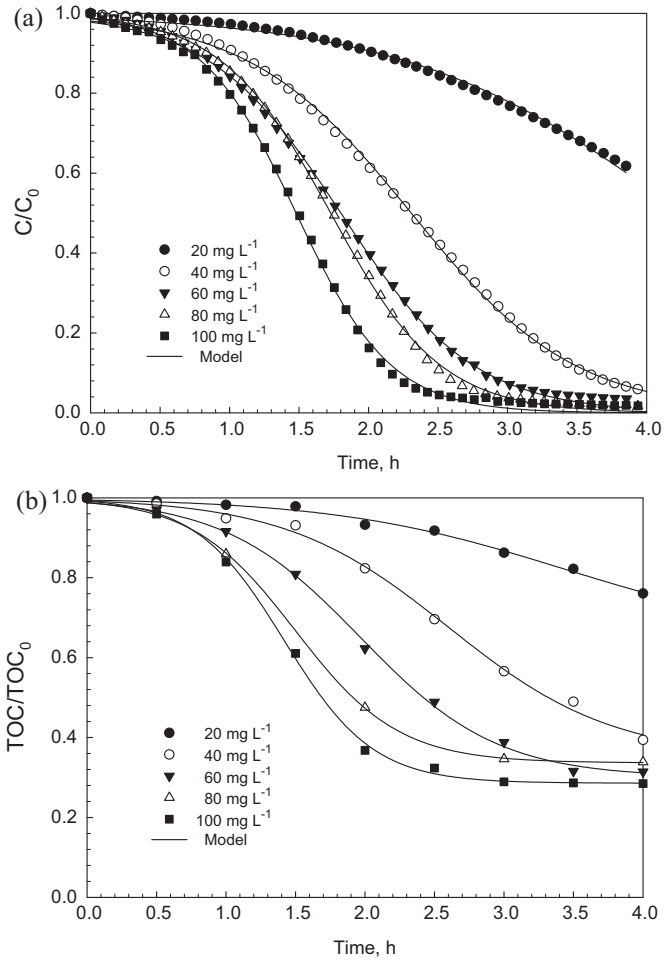

Fig. 2. Effect of the catalyst load on the dye (a) and TOC (b) degradation histories (T = 30 °C, $C_{H_2O_2}$ = 6 mM, C_{OII} = 0.1 mM). The lines represent the fitting by the model (Eqs. (1) and (2) respectively in (a) and (b) with data reported in Tables 2 and 3).

3.2. Catalyst load effect

The catalyst load was varied in a wide range, between 20 and 100 mg L^{-1}, while keeping the other parameters constant (cf. Table 2 or 3). Fig. 2a shows that the OII degradation rate decreases when lower pillared clay loads are employed, because HO• species are produced at a slower rate for the oxidation reaction. After 4 h of reaction, the OII degradation, which is complete with 100 mg L^{-1} of catalyst load, decreases to ca. 38% when the catalyst load is diminished to 20 mg L^{-1} (Fig. 2a), while the respective TOC conversion (Fig. 2b) decreases from 71.5 to 24.0% (for 100 and 20 mg L^{-1} of catalyst, respectively). Even if there is a fraction of TOC that remains in the solution, it is important to highlight the low catalyst loads employed in all cases, evidencing the high catalytic activity of the pillared clay catalyst for OII degradation and mineralization. These catalyst loads are much below typical loads employed in literature, although one obviously needs to also consider all the other operating conditions and catalyst properties. For instance, 1 g L^{-1} of a Fe-exchanged pillared beidellite catalyst, at 50 °C and pH 5, was used for degradation of phenol (initial phenol concentration of 250 mg L^{-1} and 37 mM of H_2O_2) [45] and Reactive Yellow 84 (initial dye concentration of 100 mg L^{-1} and 20 mM of H_2O_2) [36]. The same high catalyst load (1 g L^{-1}) of a laponite clay-based Fe nanocomposite was used for degradation of OII (20 °C, pH 3, 0.2 mM of OII and 9.6 mM of H_2O_2), even if in this case the process was photo-assisted with UV light [32].

3.3. H_2O_2 concentration effect

The initial H_2O_2 concentration was varied from 3.0 to 48 mM while maintaining the other parameters constant (cf. Table 2 or 3). This range was selected in accordance with the literature: 4 mM [46], 10 mM [41,47–49], 14 mM [50], and 100 mM [51] of H_2O_2 was used for degradation of the same pollutant with clay-based Fe catalysts [41,47,51] or other Fe-based materials [46,48,50]. Therefore, the H_2O_2 concentrations employed in the present study are within those employed by other authors. In fact, the H_2O_2/OII molar ratio (60) used in our typical experiments with 6.0 mM of H_2O_2 and 0.1 mM of OII is only slightly higher than the typical H_2O_2/OII molar ratio used in the literature (around 50), a wider range being studied in the present work since the H_2O_2 concentration was varied from 3.0 to 48 mM and the dye concentration from 0.02 to 0.20 mM – cf. Table 2.

Fig. 3a and b respectively show that the OII and TOC concentration histories are quite similar regardless the concentration of the oxidant agent, being achieved a complete degradation of OII and a significant TOC conversion (ca. 70%) after 4 h for all H_2O_2 concentrations tested. This behavior was not expected since the increase of the oxidant concentration usually leads to an increase in the reaction rate because more radicals are prone to be formed in the reaction. Thus, with the prepared catalyst, low amounts of H_2O_2 are enough in the CWHPO process and the performances achieved were remarkable in terms of both OII and TOC degradation, even at the lowest H_2O_2 concentration tested (3 mM).

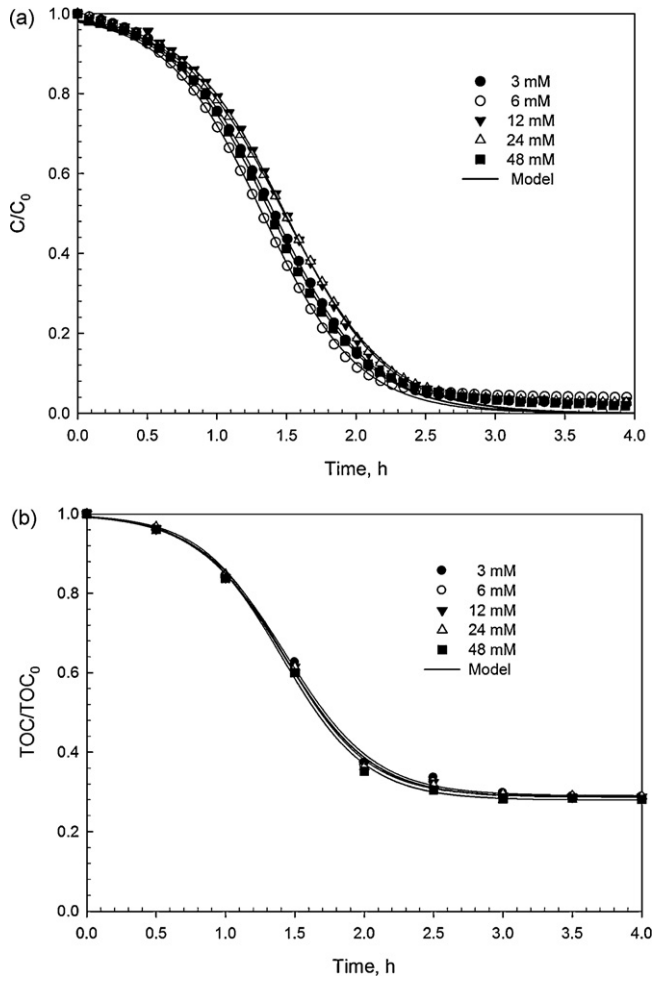

Fig. 3. Effect of the initial hydrogen peroxide concentration on the dye (a) and TOC (b) degradation histories (T = 30 °C, C_{cat} = 100 mg L^{-1}, C_{OII} = 0.1 mM). The lines represent the fitting by the model (Eqs. (1) and (2) respectively in (a) and (b) with data reported in Tables 2 and 3).

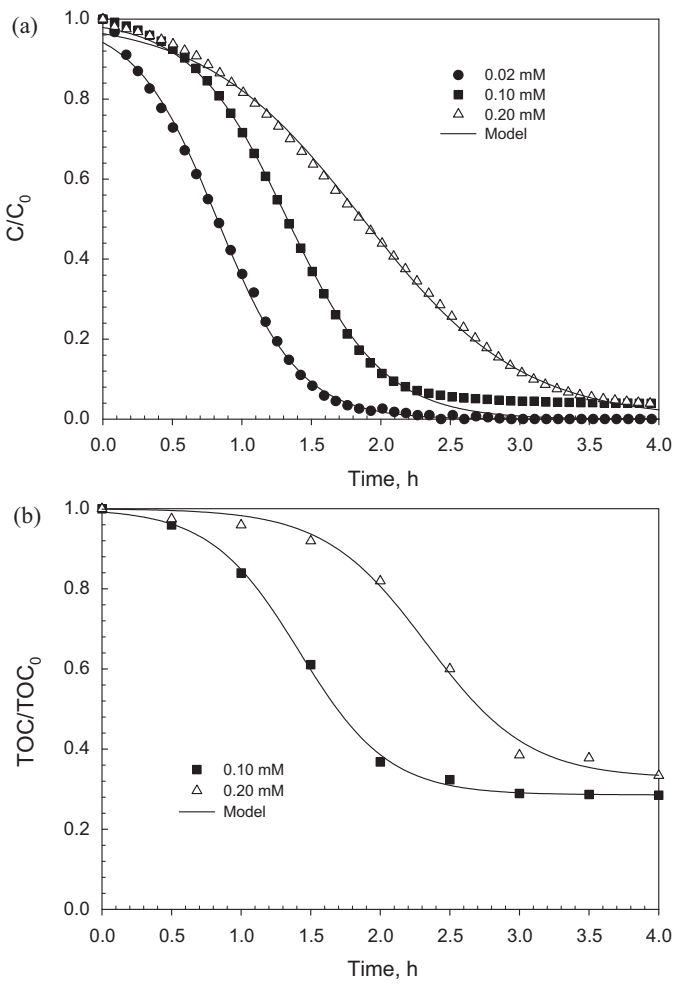

Fig. 4. Effect of the initial dye (a) and TOC (b) concentration on the degradation histories (T = 30 °C, $C_{H_2O_2}$ = 6 mM, C_{cat} = 100 mg L^{-1}). The lines represent the fitting by the model (Eqs. (1) and (2) respectively in (a) and (b) with data reported in Tables 2 and 3.)

Since the OII and TOC histories are practically the same whatever the H_2O_2 concentration tested (Fig. 3a and b, respectively), and because the degradation rate is slower in the experiments performed with a lower nominal content of iron (16 wt.%) [37], one can conclude that with the material prepared in the present work H_2O_2 is more efficiently used for both OII degradation (ca. 100%) and mineralization (ca. 70%). Therefore, at the employed conditions, the effect of the H_2O_2 concentration will be less relevant in the kinetic model that will be developed below than the other studied parameters.

3.4. Dye concentration effect

Fig. 4a and b show the OII and TOC concentration histories, respectively, normalized by the initial concentrations: C_0 in Fig. 4a (0.02, 0.10 and 0.20 mM) and TOC_0 in Fig. 4b (19 and 38 mg L^{-1} for 0.10 and 0.20 mM of C_0, respectively). For the lowest initial OII concentration tested (C_0 = 0.02 mM) the TOC concentration histories were not followed due to the large deviations associated with the analytical procedure for the TOC measurement at such low dye concentrations. Regarding the OII concentration histories, Fig. 4a shows that the higher the initial OII concentration, the higher was the time required to degrade OII completely. The same effect (decrease of the OII conversion with an increase of the initial dye concentration) was already observed by several authors [52–54]. In addition, by increasing the initial OII concentration from 0.10 up to 0.20 mM, nearly the same fraction of non-oxidizable compounds formed during the reaction was observed (Fig. 4b); the TOC remaining in the solution after 4 h was however much higher for the higher initial dye concentration tested, because TOC_0 is the double as compared with the experiment for initial OII concentration of 0.10 mM.

3.5. Catalyst stability

The amount of iron leached to the liquid phase was determined for all experiments. Fig. 5 shows the amount of iron leached with respect to the amount of iron contained in the prepared catalyst (wt.%) for different temperatures. Temperature has a strong influence on the amount of iron that is leached, namely 0.2, 0.5, 1.9 and 2.5 wt.% of iron is leached at 10, 30, 50 and 70 °C, respectively, at the end of the experiments (corresponding to final iron concentrations in the range 0.05–0.52 mg L^{-1}, which are far below the European Economic Community standards for discharge of treated waters – 2 mg L^{-1}). Therefore, in general, the temperature of 30 °C seems to be truly the optimal operating temperature if both catalyst stability (Fig. 5) and activity (Fig. 1) are considered together.

It is also important to realize that the leaching of iron at 30 °C was null after 1.5 h and only 0.07 wt.% of iron was leached after 2.0 h, while a significant OII oxidation occurred between 0.5 and 1.5 h of reaction (Fig. 1a) and the higher TOC reduction was

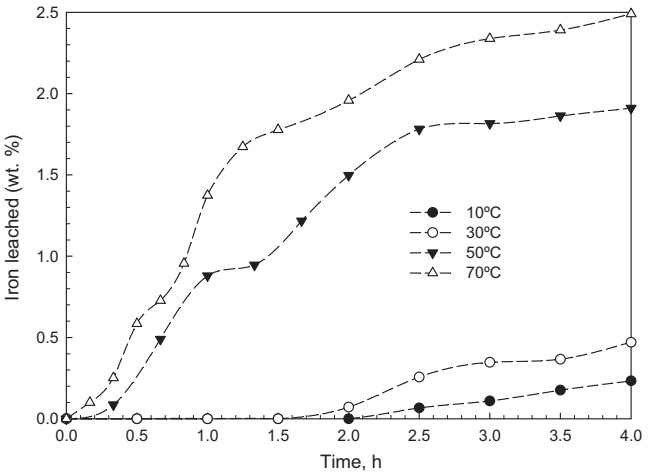

Fig. 5. Effect of temperature on the leaching of iron (C_{cat} = 100 mg L^{-1}, $C_{H_2O_2}$ = 6 mM, C_{OII} = 0.1 mM).

observed between 0.5 and 2.0 h (Fig. 1b) at the same temperature. Therefore, the OII oxidation and mineralization is not related with the presence of iron in the liquid phase, suggesting a pure heterogeneous process. In order to check possible contributions of the homogeneous reaction, a different experiment was performed in our previous work [34]: the liquid phase containing dissolved iron was separated from the solid catalyst after the first run and both OII and H_2O_2 where added once again to the recovered solution (T = 30 °C, $C_{H_2O_2}$ = 6 mM, C_{OII} = 0.1 mM), this experiment indicating that the process is essentially heterogeneous because the OII conversion was extremely low after 4 h of reaction.

In what concerns the effect of the other operating parameters studied in the present work, the leaching of iron was always lower than 0.6 wt.% after 4 h for experiments performed at 30 °C with varying doses of catalyst, H_2O_2 and dye (not shown), indicating that temperature is the main parameter affecting the catalyst stability. In our previous work [34] the leaching was also very low (1.4 wt.% after 4 h) and the catalyst (recovered by filtration) was used in four subsequent reaction cycles, the conversion decreasing only from 96 to 90%; i.e. the catalyst was very stable after 16 h of operation. Therefore, the results obtained in the present work and those previously reported indicate that saponite-based catalysts are very stable materials and that the studied degradation reaction essentially occurs by a heterogeneous (not homogeneous) process.

3.6. Development of the kinetic models

The model that was developed in our previous publication [37] to describe the OII concentration histories, Eq. (1), was based on the Fermi's function (the mirror image of the logistic function):

$$\frac{C}{C_0} = \frac{1}{1 + \exp[k(t - t^*)]} \quad (1)$$

In Eq. (1), k represents the apparent reaction rate constant (that includes the catalyst dosage – C_{cat}) and t^* is the so-called transition time, related with the OII concentration curve's inflection point. This model was developed with the aim to simultaneously describe the initial slow degradation and subsequent rapid decay of the model pollutant that is often observed for oxidation reactions using Fe-based heterogeneous catalysts and H_2O_2. The induction period observed has been commonly attributed in literature (i) to the time needed for activation of the surface iron species [35,38], or (ii) to the time required for dissolution of enough iron to promote the homogeneous Fenton reaction [55]. Since the later phenomenon is not relevant in the present work, as discussed in Section 3.5, the induction period should be attributed to the activation of the catalyst surface.

The two-step pseudo-first-order model (with two separated linear regression analysis in semi-logarithmic scale) has been used to describe the two different stages of the process [55]. However, this approach has some limitations because the normalized concentration versus time curves exhibit an inverse S-shape profile (as those shown in Figs. 1a, 2a, 3a and 4a), i.e. nearly sigmoid shape in terms of dye conversion, which have been also observed in other studies with pillared clay catalysts [38,42,43]. Other shortcomings are that the two-step pseudo-first-order model does not account for: (i) the transient period between each linear region, (ii) the non-linear behavior during the induction period, and (iii) an objective determination of each region, that in fact is subjective when applying two separated linear regressions.

Therefore, and because the degradation process does not have to follow any particular kinetics or reaction order, the main advantages associated to the model presented in Eq. (1) are that this model consists of a single semi-empirical function (mathematical simplicity) that accounts also for the dye concentration histories in the intermediate regime, using only a few adjustable parameters that have associated intuitive meanings and that can be related with the reaction conditions. Moreover, when dealing with complicated systems, involving mixtures of unknown pollutants and/or several reaction intermediates formed by complex reaction pathways during the oxidation process, the use of lumped models are forced to be used, for instance by including lumped analytical parameters such as the total organic carbon (TOC) or the chemical oxygen demand (COD) that can be derived in groups of compounds with different reactivity.

Figs. 1b, 2b, 3b and 4b show also in general an initial induction period characterized by a slow TOC reduction, which is related to the initial activation of the catalyst (because an induction period was also observed in the OII degradation histories) and possibly to some organic compounds that are formed at a slow rate. Then, a period is observed where the TOC decreases sharply due to the fast degradation of OII and other intermediates into the final desired end products, such as CO_2 and H_2O, and finally a period is noticed where a fraction of non-oxidizable compounds remain in the solution (plateau) contributing to the TOC content at the end of the experiments.

According to common nomenclature in literature, chemical species in AOPs can be classified into unstable pollutants that are easily oxidized, named as "A", intermediate species, designed as "B", final end products, such as CO_2 and H_2O, represented by "C", and, in some cases, some pollutants or reaction intermediate compounds that are not oxidized under certain operating conditions may be classified in a separate group designed as "D" (refractory substances) [44]. The models usually presented in the literature may be divided into two main groups: one facing the oxidation treatment as a sequential process in time and another assuming that the various reaction pathways are possible to occur simultaneously. The kinetic parameters are generally obtained by taking into account first-order kinetic reactions with respect to the TOC concentration.

In our particular case, "A" corresponds to OII (t = 0 min), "B" to intermediate compounds that are easily degraded and that are formed at intermediate reaction times, while "D" represents those non-oxidizable compounds that will not react under the operating conditions used and that are responsible for the TOC fraction remaining in the solution after 4 h. Some of these possible reaction intermediates are proposed in our previous publication [34]. The end products "C" and the non-oxidizable compounds "D" are then supposed to be the final products of the oxidation treatment. Therefore, pollutants with different reactivities are involved in the process, and aiming to develop a kinetic model that could represent

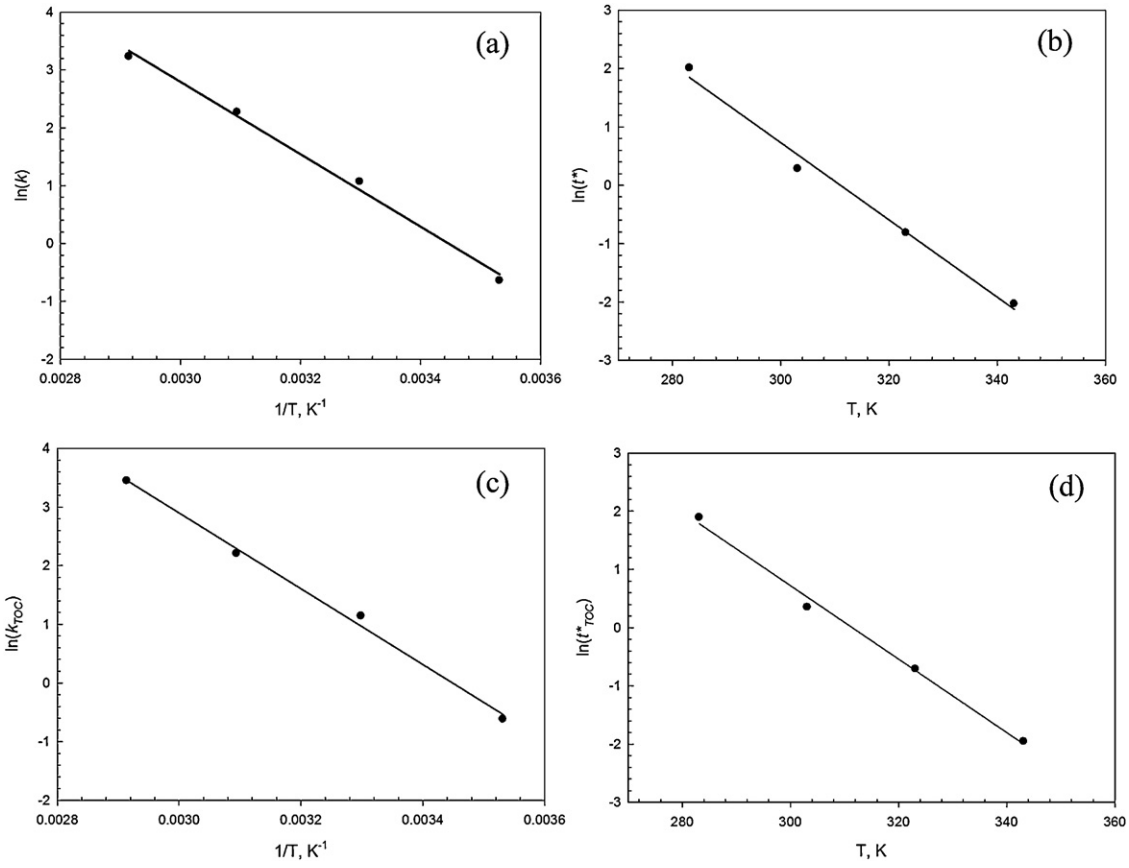

Fig. 6. Arrhenius plot for the apparent rate constants obtained for the dye (a) and TOC (c) degradation histories, and effect of temperature on the respective transition times (b, d); for the other conditions please refer to Tables 2 and 3, respectively. The lines represent the linear regression fittings; r^2: 0.9945 (a); 0.9896 (b); 0.9952 (c); 0.9945 (d).

the oxidation of the TOC lumped concentration, including OII and respective reaction intermediates, the previous model based on the Fermi's equation, Eq. (1), was upgraded in the present work with the aim to describe the obtained TOC concentration histories. Different approaches were considered which allowed concluding that the model represented in Eq. (2) is the most suitable to represent the data:

$$\frac{\mathrm{TOC}}{\mathrm{TOC}_0} = \frac{1 - z_{\mathrm{TOC}}}{1 + \exp[k_{\mathrm{TOC}}(t - t^*_{\mathrm{TOC}})]} + z_{\mathrm{TOC}} \quad (2)$$

where k_{TOC} represents the apparent reaction rate constant with respect to the TOC concentration (and also includes the catalyst dosage, C_{cat}), t^*_{TOC} corresponds to the transition time related to the TOC concentration curve's inflection point, and z_{TOC} represents the fraction of non-oxidizable compounds that are formed during the reaction, i.e. a variation of "D" species that was applied to the model developed with the Fermi's equation:

$$z_{\mathrm{TOC}} = \frac{\mathrm{TOC}_{\text{non-oxidizable}}}{\mathrm{TOC}_0} \quad (3)$$

Eq. (2) can be rearranged with Eq. (3) yielding Eq. (4), which clearly represents a single and simple semi-empirical function accounting for the conversion of the oxidizable reaction compounds ($\mathrm{TOC}_{\text{oxidizable}} = \mathrm{TOC} - \mathrm{TOC}_{\text{non-oxidizable}}$).

$$\frac{\mathrm{TOC}_0 - \mathrm{TOC}}{\mathrm{TOC}_0} = \frac{(\mathrm{TOC} - \mathrm{TOC}_{\text{non-oxidizable}})}{\mathrm{TOC}_0} \times \exp[k_{\mathrm{TOC}}(t - t^*_{\mathrm{TOC}})] \quad (4)$$

3.7. Application of the kinetic models to describe the dye and TOC degradation histories

The models presented in Eqs. (1) and (2) were fitted to the normalized OII (C/C_0) and TOC ($\mathrm{TOC}/\mathrm{TOC}_0$) concentration histories, respectively, and the values of the model parameters (k and t^* shown in Table 2, and k_{TOC}, t^*_{TOC} and z_{TOC} in Table 3) were obtained after regression (Figs. 1–4). The Marquardt-Levenberg algorithm that seeks the values of the parameters that minimize the sum of the squared differences between observed and predicted values of the dependent variable (tolerance = 1×10^{-10}) was used. The coefficients of variation (CV), expressed as a percentage (k_{CV}, t^*_{CV}, $k_{\mathrm{CV,TOC}}$, $t^*_{\mathrm{CV,TOC}}$ and $z_{\mathrm{CV,TOC}}$), are also presented in Tables 2 and 3. The asymptotic standard error of each parameter measures the uncertainties in the estimates of the regression coefficient (analogous to the standard error of the mean). CV(%) is the normalized version of this error (CV (%) = Standard Error × 100/parameter value).

A good agreement of the models (Eqs. (1) and (2)) to the experimental data was observed in general for all the operating conditions tested, in terms of both OII and TOC concentration histories, as demonstrated by the fitting of the models to the experimental data in Figs. 1–4. This is also corroborated by the respective CV(%) values presented in Tables 2 and 3, as well as by the coefficients of determination presented in Table 2 (r^2 values in the range 0.9743–0.9994) and in Table 3 (r^2 values in the range 0.9906–0.9996).

In what concerns the effect of the temperature (Fig. 1), both apparent kinetic constants (k and k_{TOC}) markedly increased with the increase of this parameter (Tables 2 and 3, respectively) and followed an Arrhenius behavior; k in Fig. 6a and k_{TOC} in Fig. 6c, yielding apparent activation energies of 52 and 54 kJ mol^{-1}, respectively (Tables 2 and 3). A clear meaning cannot be attributed to

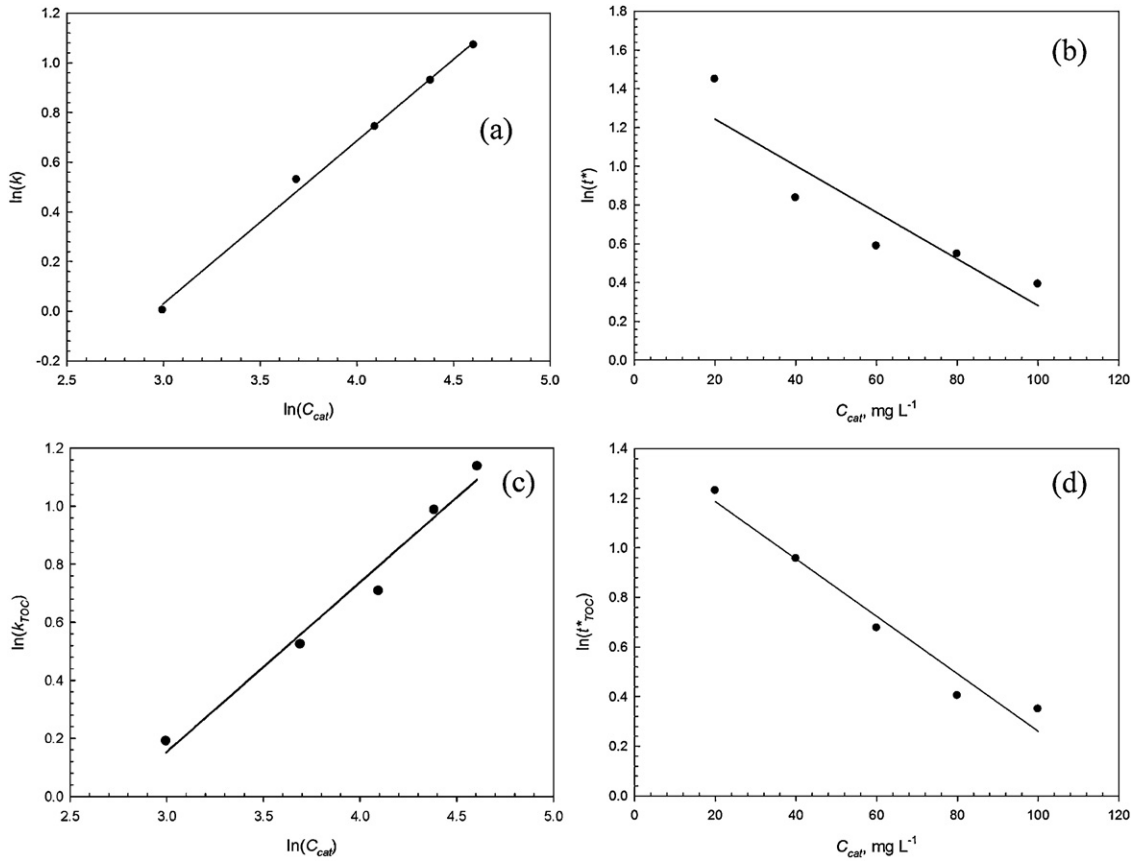

Fig. 7. Effect of the catalyst load on the apparent rate constants of the models fitted to dye (a) and TOC (c) degradation histories, and on the respective transition times (b, d); for the other conditions please refer to Tables 2 and 3. The lines represent the linear regression fittings; r^2: 0.9957 (a); 0.8363 (b); 0.9777 (c); 0.9642 (d).

these parameters under the complex conditions of the reaction in the CWHPO process. Even so, the apparent activation energy determined for OII is similar to the one found in our previous publication [37], namely 47 kJ mol^{-1}, as well as to values already reported in literature for the same dye pollutant, namely 56 kJ mol^{-1} when using carbon-Fe catalysts and a pseudo-first order reaction rate [30] and 47 kJ mol^{-1} for a photo-assisted process with a Fe/C structured catalyst [56].

In addition, the transition time decreases, for both OII and TOC concentration histories, by increasing the temperature from 10 to 70 °C (respectively, t^* from 7.45 to 0.13 h in Table 2 and t^*_{TOC} from 6.64 to 0.14 h in Table 3). A clear correlation was obtained in both cases when plotting this effect in a semi-logarithmic scale, for t^* in Fig. 6b and t^*_{TOC} in Fig. 6d. These regressions could be helpful to determine the t^* corresponding to intermediate temperatures, between 10 and 70 °C, other authors presenting similar approaches [38]. In general, t^* and t^*_{TOC} have similar values (1.33 and 1.42, 0.44 and 0.49, 0.13 and 0.14 h, respectively for 30, 50 and 70 °C). These results indicate that the marked decrease in the TOC concentration is mainly related with the sharp decrease in the equivalent OII concentration for each temperature tested.

Significant differences between t^* and t^*_{TOC} (7.45 and 6.64 h, respectively) were only observed when the regression was applied to the experimental data obtained at the lowest temperature (10 °C), probably because in this case the reaction proceeds very slowly and, consequentially, it is not possible within 4 h to observe the transition between the induction period and the fast oxidation reaction, being the estimation for t^* and t^*_{TOC} not so good as those obtained at higher temperatures where the transition is clear. Even so, it was possible to estimate t^*_{TOC} because the fitting was obtained considering a further experimental value at 10 °C after the first 4 h, i.e. TOC/TOC$_0$ of 0.39 after 23 h, as previously described.

Table 3 also shows the TOC fraction of non-oxidizable compounds predicted by the model for each temperature (z_{TOC} = 0.39, 0.29, 0.22 and 0.19 at 10, 30, 50 and 70 °C, respectively), which represent very well the experimental data (0.39, 0.29, 0.20, and 0.17 at 10, 30, 50 and 70 °C, respectively, Fig. 1b, although at 10 °C it refers to the experimental value after 23 h). Thus, it is clear that the fraction of the initial TOC remaining at the end of the experiment decreases with the increase of the temperature.

Regarding the effect of the catalyst load (Table 2), once again the fittings, Eqs. (1) and (2), matched well the data for both OII (Fig. 2a) and TOC (Fig. 2b) concentration histories, respectively, k and k_{TOC} increasing with the catalyst load. In addition, the logarithmic plot of k (Fig. 7a) and k_{TOC} (Fig. 7c) versus the catalyst load leads to apparent reaction orders of 0.66 (Table 2) and 0.58 (Table 3), the first being slightly higher than the one determined in our previous work (0.59) with a lower nominal iron content of 16 wt.% in the catalyst [37]. These fractional values are a mirror of the complex reaction process.

In what concerns the time required to achieve 50% of conversion, either in terms of OII or oxidizable TOC, it can be observed that the higher is the catalyst load, the shorters are the respective periods, i.e. t^* (Table 2) and t^*_{TOC} (Table 3), both parameters decreasing nearly exponentially with C_{cat} (Fig. 7b and d, respectively). For the fraction of non-ozidizable compounds (z_{TOC}), the predicted TOC values at the end of the experiments are very similar (0.32 ± 0.03), as expected, and only for the lowest catalyst load (20 mg L^{-1}) there is a clear deviation to 0.65 because the reaction is very slow and

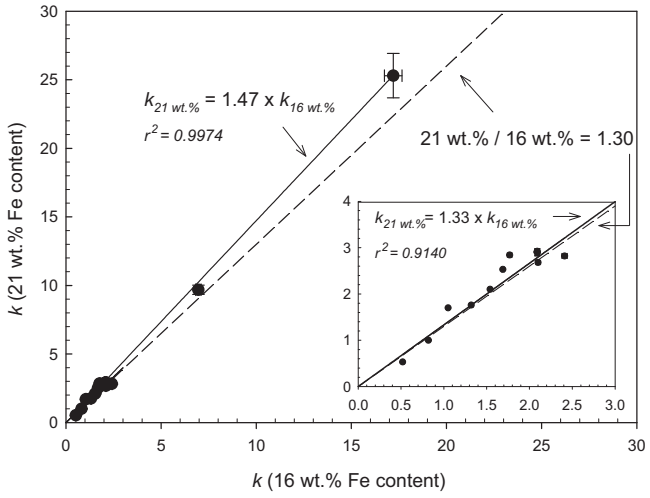

Fig. 8. Comparison between the apparent rate constants obtained at similar operating conditions with pillared saponite clay catalysts consisting of 21 and 16 wt.% of iron content.

the experimental data obtained within 4 h does not illustrate the S-shaped transient curve. In fact, the respective coefficient of variation is quite high ($z_{CV,TOC}$ = 10.3%) in this particular experiment, as well as the t^* obtained for 20 mg L^{-1} deviates from those t^* obtained at higher catalyst loads (Fig. 7b), suggesting that the prediction of the model is not really good in the experiment with the lower catalyst load (20 mg L^{-1}) due to the low reaction rate associated with this experiment.

Very good fits to the experimental data were also obtained for the experiments performed with different H_2O_2 concentrations (Fig. 3a), but in this case the effect on k and k_{TOC} is practically negligible ($2.79 \pm 0.11\ h^{-1}$ in Table 2 and $3.20 \pm 0.09\ h^{-1}$ in Table 3, respectively). The same occurs for the other parameters: t^* and t^*_{TOC} (1.41 ± 0.08 h in Table 2 and 1.41 ± 0.02 h in Table 3) and z_{TOC} (0.28–0.29 in Table 3).

The models were also good to fit the data obtained for different initial OII concentrations (cf. Fig. 4a and b, and r^2 values in Tables 2 and 3, respectively, for OII and TOC concentration histories). Higher OII concentrations have a negative effect on k, which decreases from 3.38 to 1.76 h^{-1} (Table 2) when the OII concentration is increased by a factor of ten (from 0.02 up to 0.20 mM) while t^* increases from 0.82 up to 1.87 h. The same trends were observed with respect to the TOC related data (k_{TOC} and t^*_{TOC} in Table 3), z_{TOC} values (0.31 ± 0.02) being within the range of those obtained at 30 °C.

Aiming to compare the results obtained in the present work with those previously reported [37] in terms of the apparent reaction rate constants for pillared clay catalysts with different nominal iron contents, each k value obtained for a nominal iron content of 21 wt.% ($k_{21\ wt.\%}$) was plotted against the respective k value obtained at similar experimental conditions but using a catalyst with a nominal iron content of 16 wt.% ($k_{16\ wt.\%}$) [37]. The results are shown in Fig. 8 where each data point corresponds to a given rate constant obtained under specific operating conditions. It is very interesting to note that the wt.% ratio of iron content between both materials is 1.30 (21 wt.% divided by 16 wt.%), while the ratio obtained by linear regression of these k values is only slightly higher, i.e. 1.47. In fact, if the two highest k values are not considered in this analysis (inset of Fig. 8) both values match quite well, i.e. the ratio of 1.30 with the value obtained by linear regression (1.33), suggesting that the apparent rate constants, and inherently the reaction extent, are proportional to the iron content in the catalyst.

4. Conclusions

The Fenton-like parametric study performed, using the pillared saponite clay containing 21 wt.% of Fe for Orange II degradation, allowed concluding that:

- Among all the variables tested, temperature revealed to have a more pronounced effect, increasing reaction rate (dye degradation and mineralization) but also iron leaching from the support. However, in all cases, iron leaching was always <2.5%, which was reached at the highest temperature of 70 °C. This yielded an iron content in solution of ca. 0.5 mg L^{-1}, which still complies with EU legislated standards. Besides, these results put into evidence the stability of the catalyst, and that the process is essentially heterogeneous, not homogeneous, most of the pollutant degradation occurring before any leaching of the active phase.
- In the range of conditions tested, the amount of catalyst accelerates the oxidation, as expected, while the dose of oxidant showed negligible effect in the dye and TOC concentration histories; so, H_2O_2 concentration had no effect in the model parameters.

The semi-empirical model, based on the Fermi's equation, provided very good fittings for all CWHPO experiments in terms of dye concentration histories. Besides, the lumped model developed in the present work, also based on the Fermi's equation, was able to predict the evolution of the TOC concentration histories, showing very good adherence to the experimental data. Correlations established between the model parameters and the operating conditions allow obtaining the model coefficients at any conditions within the range of the parametric study. The computed kinetic constants are in agreement with that of a previous work where the same type of catalyst was employed, if the different load of Fe is taken into account. Therefore, one can predict the performance reached by any similar catalyst, even if containing a different iron load.

Acknowledgements

Financial support for this work was partially provided by project PEst-C/EQB/LA0020/2011, financed by FEDER through COMPETE – Programa Operacional Factores de Competitividade –, by FCT – Fundação para a Ciência e a Tecnologia –, and by the University of Porto with the contribution of Santander Totta. AMTS acknowledges financial support from POCI/N010/2006.

References

[1] G. McMullan, C. Meehan, A. Conneely, N. Kirby, T. Robinson, P. Nigam, I.M. Banat, R. Marchant, W.F. Smyth, Applied Microbiology and Biotechnology 56 (2001) 81–87.
[2] C.I. Pearce, J.R. Lloyd, J.T. Guthrie, Dyes and Pigments 58 (2003) 179–196.
[3] J.-W. Lee, S.-P. Choi, R. Thiruvenkatachari, W.-G. Shim, H. Moon, Dyes and Pigments 69 (2006) 196–203.
[4] X.S. Wang, Y. Zhou, Y. Jiang, C. Sun, Journal of Hazardous Materials 157 (2008) 374–385.
[5] R. Songur, E. Bayraktar, U. Mehmetoglu, World Academy of Science, Engineering and Technology 59 (2011) 1999–2003.
[6] G. Bayramoglu, B. Altintas, M.Y. Arica, Chemical Engineering Journal 152 (2009) 339–346.
[7] M.-X. Zhu, L. Lee, H.-H. Wang, Z. Wang, Journal of Hazardous Materials 149 (2007) 735–741.
[8] B. Merzouk, B. Gourich, A. Sekki, K. Madani, C. Vial, M. Barkaoui, Chemical Engineering Journal 149 (2009) 207–214.
[9] M. Eyvaz, M. Kirlaroglu, T.S. Aktas, E. Yuksel, Chemical Engineering Journal 153 (2009) 16–22.
[10] F. Gosetti, V. Gianotti, S. Angioi, S. Polati, E. Marengo, M.C. Gennaro, Journal of Chromatography A 1054 (2004) 379–387.
[11] K. Kumar, S. Saravana Devi, K. Krishnamurthi, S. Gampawar, N. Mishra, G.H. Pandya, T. Chakrabarti, Bioresource Technology 97 (2006) 407–413.
[12] F.J. Beltran, J.M. Encinar, J.F. Garcia-Araya, Water Research 24 (1990) 1309–1316.
[13] C.-H. Wu, C.-Y. Kuo, C.-L. Chang, Reaction Kinetics and Catalysis Letters 91 (2007) 161–168.

[14] A.K. Kondru, P. Kumar, S. Chand, Journal of Hazardous Materials 166 (2009) 342–347.
[15] H.T. Gomes, S.M. Miranda, M.J. Sampaio, A.M.T. Silva, J.L. Faria, Catalysis Today 151 (2010) 153–158.
[16] C. Hu, J.C. Yu, Z. Hao, P.K. Wong, Applied Catalysis B: Environmental 46 (2003) 35–47.
[17] W. Baran, A. Makowski, W. Wardas, Dyes and Pigments 76 (2008) 226–230.
[18] M.A. Sanromán, M. Pazos, M.T. Ricart, C. Cameselle, Chemosphere 57 (2004) 233–239.
[19] A.L. Barros, T.M. Pizzolato, E. Carissimi, I.A.H. Schneider, Minerals Engineering 19 (2006) 87–90.
[20] J.-H. Sun, S.-P. Sun, G.-L. Wang, L.-P. Qiao, Dyes and Pigments 74 (2007) 647–652.
[21] N. Modirshahla, M.A. Behnajady, F. Ghanbary, Dyes and Pigments 73 (2007) 305–310.
[22] T. Kurbus, A.M. Le Marechal, D.B. Voncina, Dyes and Pigments 58 (2003) 245–252.
[23] T. Kurbus, Y.M. Slokar, A.M. Le Marechal, Dyes and Pigments 54 (2002) 67–78.
[24] Q. Chen, P. Wu, Z. Dang, N. Zhu, P. Li, J. Wu, X. Wang, Separation and Purification Technology 71 (2010) 315–323.
[25] J. Herney-Ramirez, M.A. Vicente, L.M. Madeira, Applied Catalysis B: Environmental 98 (2010) 10–26.
[26] C. Walling, Accounts of Chemical Research 8 (1975) 125–131.
[27] M. Neamtu, C. Zaharia, C. Catrinescu, A. Yediler, M. Macoveanu, A. Kettrup, Applied Catalysis B: Environmental 48 (2004) 287–294.
[28] F. Duarte, L.M. Madeira, Separation Science & Technology 45 (2010) 1512–1520.
[29] T.L.P. Dantas, V.P. Mendonça, H.J. José, A.E. Rodrigues, R.F.P.M. Moreira, Chemical Engineering Journal 118 (2006) 77–82.
[30] J.H. Ramirez, F.J. Maldonado-Hódar, A.F. Pérez-Cadenas, C. Moreno-Castilla, C.A. Costa, L.M. Madeira, Applied Catalysis B: Environmental 75 (2007) 312–323.
[31] F. Duarte, F.J. Maldonado-Hódar, L.M. Madeira, Applied Catalysis B: Environmental 103 (2011) 109–115.
[32] J. Feng, X. Hu, P.L. Yue, H.Y. Zhu, G.Q. Lu, Chemical Engineering Science 58 (2003) 679–685.
[33] O. Sze Nga Sum, J. Feng, X. Hu, P. Lock Yue, Chemical Engineering Science 59 (2004) 5269–5275.
[34] J.H. Ramirez, C.A. Costa, L.M. Madeira, G. Mata, M.A. Vicente, M.L. Rojas-Cervantes, A.J. López-Peinado, R.M. Martín-Aranda, Applied Catalysis B: Environmental 71 (2007) 44–56.
[35] M.N. Timofeeva, S.T. Khankhasaeva, S.V. Badmaeva, A.L. Chuvilin, E.B. Burgina, A.B. Ayupov, V.N. Panchenko, A.V. Kulikova, Applied Catalysis B: Environmental 59 (2005) 243–248.
[36] C. Catrinescu, M. Neamtu, J. Miehe-Brendlé, M.G. Garcia, A. Kettrup, in: M. Suárez, M.A. Vicente, V. Rives, M.J. Sánchez (Eds.), Materiales Arcillosos: de la Geologia a las Nuevas Aplicaciones, Sociedad Española de Arcillas, Salamanca, 2006, pp. 87–98.
[37] J. Herney-Ramirez, A.M.T. Silva, M.A. Vicente, C.A. Costa, L.M. Madeira, Applied Catalysis B: Environmental 101 (2011) 197–205.
[38] M. Luo, D. Bowden, P. Brimblecombe, Applied Catalysis B: Environmental 85 (2009) 201–206.
[39] J. Herney-Ramirez, M. Lampinen, M.A. Vicente, C.A. Costa, L.M. Madeira, Industrial & Engineering Chemistry Research 47 (2008) 284–294.
[40] J. Herney-Ramírez, L.M. Madeira, in: A. Gil, S.A. Korili, R. Trujillano, M.A. Vicente (Eds.), Pillared Clays and Related Catalysts, 1st ed., Springer, 2010, pp. 129–165.
[41] J. Feng, X. Hu, P.L. Yue, Water Research 40 (2006) 641–646.
[42] E. Guélou, J. Barrault, J. Fournier, J.-M. Tatibouët, Applied Catalysis B: Environmental 44 (2003) 1–8.
[43] J. Barrault, M. Abdellaoui, C. Bouchoule, A. Majesté, J.M. Tatibouët, A. Louloudi, N. Papayannakos, N.H. Gangas, Applied Catalysis B: Environmental 27 (2000) L225–L230.
[44] A.M.T. Silva, R.M. Quinta-Ferreira, J. Levec, Industrial & Engineering Chemistry Research 42 (2003) 5099–5108.
[45] C. Catrinescu, C. Teodosiu, M. Macoveanu, J. Miehe-Brendlé, R. Le Dred, Water Research 37 (2003) 1154–1160.
[46] S. Silva Martínez, J. Vergara Sánchez, J.R. Moreno Estrada, R. Flores Velásquez, Solar Energy Materials and Solar Cells 95 (2011) 2010–2017.
[47] J. Chen, L. Zhu, Chemosphere 65 (2006) 1249–1255.
[48] J. Feng, R.S.K. Wong, X. Hu, P.L. Yue, Catalysis Today 98 (2004) 441–446.
[49] J. Feng, X. Hu, P.L. Yue, Environmental Science & Technology 38 (2003) 269–275.
[50] F.L.Y. Lam, X. Hu, Catalysis Communications 8 (2007) 2125–2129.
[51] J. Feng, X. Hu, P.L. Yue, S. Qiao, Separation and Purification Technology 67 (2009) 213–217.
[52] J. Guo, M. Al-Dahhan, Industrial & Engineering Chemistry Research 42 (2003) 2450–2460.
[53] A. Pintar, J. Levec, Journal of Catalysis 135 (1992) 345–357.
[54] D. Tabet, M. Saidi, M. Houari, P. Pichat, H. Khalaf, Journal of Environmental Management 80 (2006) 342–346.
[55] T. Gordon, A. Marsh, Catalysis Letters 132 (2009) 349–354.
[56] T. Yuranova, O. Enea, E. Mielczarski, J. Mielczarski, P. Albers, J. Kiwi, Applied Catalysis B: Environmental 49 (2004) 39–50.